nature photonics

SUPPLEMENTARY INFORMATION

DOI: 10.1038/NPHOTON.2017.117

In the format provided by the authors and unedited.

Counter-propagating solitons in microresonators

Qi-Fan Yang*, Xu Yi*, Ki Youl Yang, and Kerry Vahala†
T. J. Watson Laboratory of Applied Physics, California Institute of Technology, Pasadena, California 91125, USA.
*These authors contributed equally to this work.
†Corresponding author: vahala@caltech.edu

I. TUNING OF RELATIVE RATE AND OFFSET

To achieve independent control of the counter-propagating (CP) soliton repetition rate difference and the pump frequency offset, we employ a two-step tuning protocol. First, the frequency difference of the two AOMs (see fig. 1b), which is exactly the soliton frequency offset $\Delta\nu$, is set to a desired value. Second, the clockwise pump to cavity resonance detuning frequency is tuned by adjusting the pump laser locking setpoint using the servo control. This allows the continuous tuning of repetition rate difference Δf. A plot of this process based on eq. (5) in the Methods section is provided in fig. S1.

II. LOCKING OF COUNTER PROPAGATING SOLITONS AT THE SAME REPETITION RATE

In this section the mechanism of soliton repetition rate locking to an identical rate is discussed (Fig. 2 within main text). Backscattering of pump light from the tapered fibre used to couple power to the resonator is believed to induce this locking. For example, consider taper backscattering of the clockwise (CW) pump. The backscattered pump light propagates with the counter-clockwise (CCW) soliton in the resonator. The CCW soliton and the backscattered CW pump experience four-wave-mixing that creates sidebands on the CCW soliton. These side bands lie at frequencies which are very close to the CW soliton. Backscatter coupling of these sidebands (and similar sidebands produced by taper backscattering of the CCW pump) causes the soliton repetition rates to lock through injection locking. This process is described schematically in fig. S2(a).

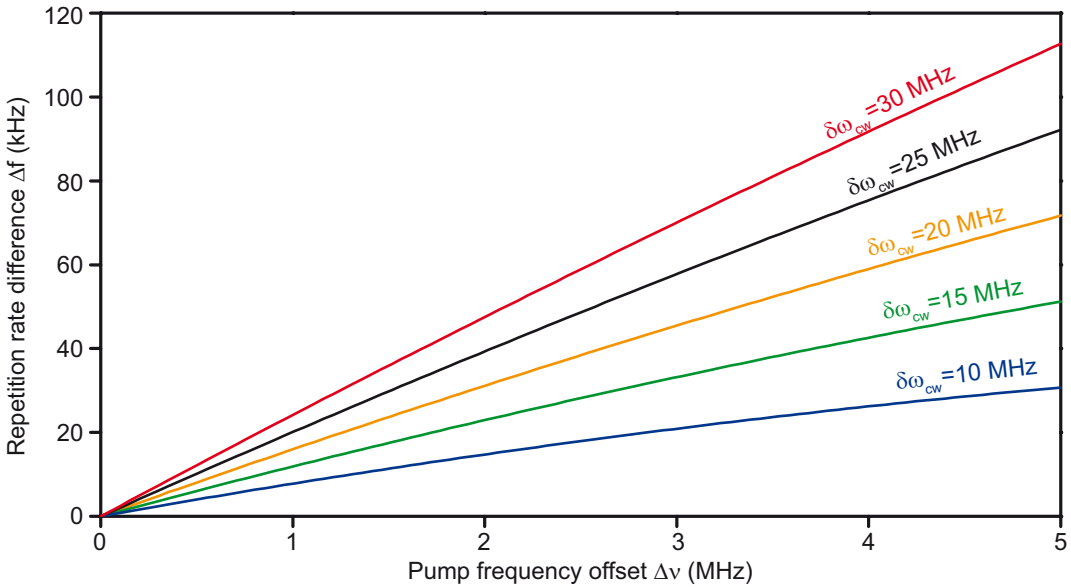

FIG. S1: **Independent tuning of CP soliton repetition rate and pump frequency offset.** Calculated CP soliton repetition rate difference versus pump frequency offset at different pump-cavity detuning frequencies in clockwise direction based on eq. (5) in the Methods Section.

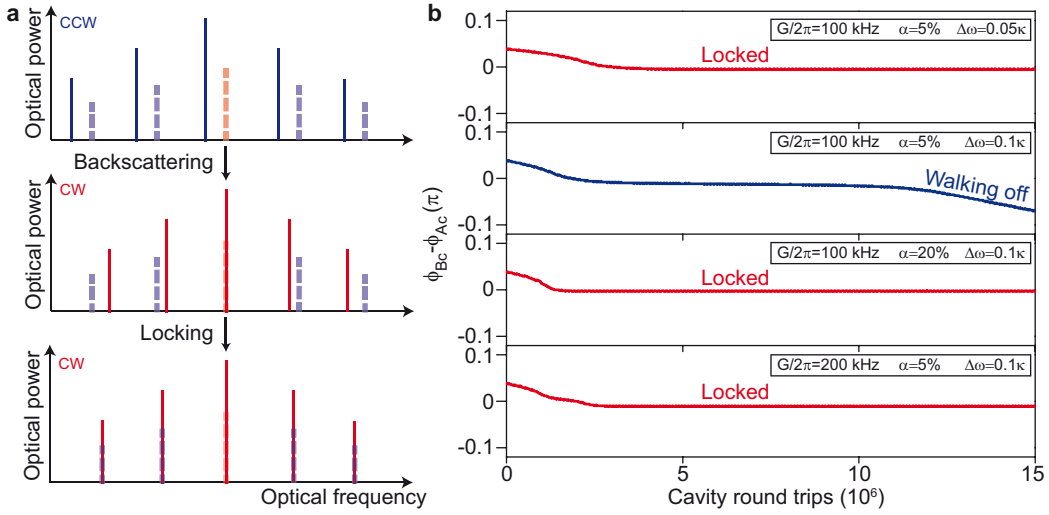

FIG. S2: **Mechanism of CP soliton synchronization. a,** Rate locking occurs when the repetition rates of A_p and B_p are injection-locked by the backscattering of B_b and A_b, respectively. The upper panel shows four-wave-mixing sidebands (dashed blue lines) on the comb lines of the CCW soliton (solid blue lines). These are created by taper backscattering of the CW pump. These sidebands are subsequently backscattered within the resonator into the CW direction (middle panel), where they (and their CW counter-parts) induce injection locking of the CW and CCW solitons (lower panel). **b,** Simulation of CP soliton repetition rate locking. ϕ_{Ac} and ϕ_{Bc} are the peak position of solitons in CW and CCW rotation frames, respectively. See text for discussion of four panels.

Such a dual-pumped microresonator with bacscattering can be described by

$$\frac{\partial A(\phi,t)}{\partial t} = -(\frac{\kappa}{2} + i\delta\omega_A)A + i\frac{D_2}{2}\frac{\partial^2 A}{\partial\phi^2} + F_A + \sqrt{\alpha}F_B e^{i\Delta\omega t} + igA(\phi,t)\int_0^\infty R(\phi'/D_1)|A(t,\phi+\phi')|^2 d\phi'/D_1, \quad \text{(S1)}$$

where F_A (F_B) is the pump field for the soliton described by amplitude A (B), α denotes the taper back-reflection portion of the pump power, κ is the decay rate of the soliton field, $\delta\omega_A$ is the frequency detuning of the pump field relative to the cavity mode being pumped, and D_2 is the second order dispersion. The last term includes both the Kerr and Raman nonlinearity[1,2]. The nonlinear response term $R(t)$ has the form[1]

$$R(t) = (1-f_R)\delta(t) + f_R h_R(t), \quad \text{(S2)}$$

where the delay in electrical response is ignored and $h_R(t)$ accounts for the Raman response. The Raman fraction for silica ($f_R = 0.18$) is assumed.

By expanding the intracavity field at two pump frequencies as $A = A_p + A_b e^{i\Delta\omega t}$ where A_p is the amplitude for the existing soliton and A_b is the field that forms in response to the backscattered pump field, we can derive the following coupled amplitude equations[1,2]

$$\frac{\partial A_p(\phi,t)}{\partial t} = -(\frac{\kappa}{2} + i\delta\omega_A)A_p + i\frac{D_2}{2}\frac{\partial^2 A_p}{\partial\phi^2} + F_A + ig[|A_p|^2 + (2-f_R)|A_b|^2]A_p + ig\tau_R D_1 A_p\frac{\partial(|A_p|^2+|A_b|^2)}{\partial\phi}, \quad \text{(S3)}$$

$$\frac{\partial A_b(\phi,t)}{\partial t} = -(\frac{\kappa}{2} + i\delta\omega_B)A_b + i\frac{D_2}{2}\frac{\partial^2 A_b}{\partial\phi^2} + \sqrt{\alpha}F_B + ig[|A_b|^2 + (2-f_R)|A_p|^2]A_b + ig\tau_R D_1 A_b\frac{\partial(|A_p|^2+|A_b|^2)}{\partial\phi}, \quad \text{(S4)}$$

where the Raman gain between the two fields has been ignored as $\Delta\omega$ is much smaller than the material's Raman shift. $\tau_R \sim 2.4$ fs is the Raman shock time in silica[1–3].

As $\alpha \ll 1$, we assume that the backscattered field is a perturbation to the existing soliton field ($|A_b| \ll |A_p|$). The existing soliton therefore maintains propagation as a soliton. Next, the intracavity backscattering is added (see equations in Methods Section) by including coupling from the existing soliton propagating in the opposing direction. The amplitude of this soliton is denoted by B_p and its weak pump backscattering component is denoted by B_b such that $B = B_p + B_b e^{-i\Delta\omega t}$. The complete coupled equations are given by,

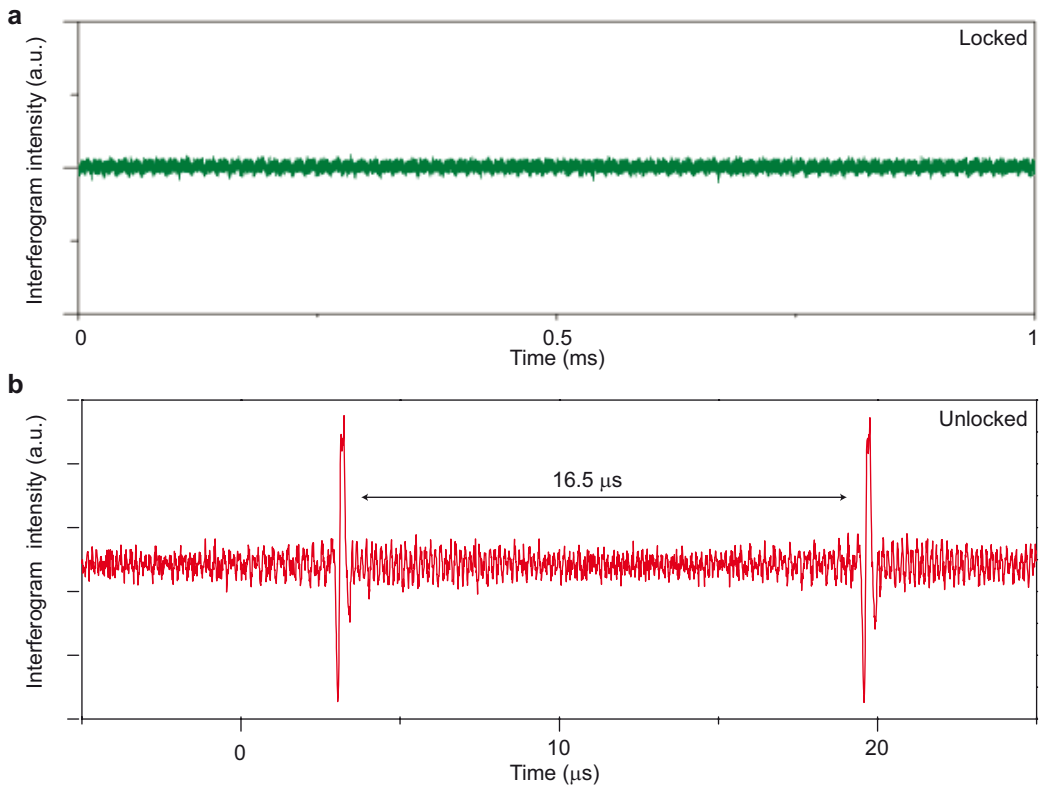

FIG. S3: **a,** Interferogram of the CP solitons when the repetition rates are locked. The soliton offset $\Delta\nu$ is 77 kHz. **b,** Interferogram of the CP solitons when the repetition rates are unlocked. Taken from fig. 2c of main text. The soliton offset $\Delta\nu$ is 3.9 MHz.

$$\frac{\partial A_p(\phi,t)}{\partial t} = -(\frac{\kappa}{2}+i\delta\omega_A)A_p+i\frac{D_2}{2}\frac{\partial^2 A_p}{\partial\phi^2}+F_A+ig[|A_p|^2+(2-f_R)|A_b|^2]A_p+ig\tau_R D_1 A_p\frac{\partial(|A_p|^2+|A_b|^2)}{\partial\phi}+iGB_b, \quad \text{(S5)}$$

$$\frac{\partial A_b(\phi,t)}{\partial t} = -(\frac{\kappa}{2}+i\delta\omega_B)A_b+i\frac{D_2}{2}\frac{\partial^2 A_b}{\partial\phi^2}+\sqrt{\alpha}F_B+ig[|A_b|^2+(2-f_R)|A_p|^2]A_b+ig\tau_R D_1 A_b\frac{\partial(|A_p|^2+|A_b|^2)}{\partial\phi}+iGB_p. \quad \text{(S6)}$$

$$\frac{\partial B_p(\phi,t)}{\partial t} = -(\frac{\kappa}{2}+i\delta\omega_B)B_p+i\frac{D_2}{2}\frac{\partial^2 B_p}{\partial\phi^2}+F_B+ig[|B_p|^2+(2-f_R)|B_b|^2]B_p+ig\tau_R D_1 B_p\frac{\partial(|B_p|^2+|B_b|^2)}{\partial\phi}+iG^*A_b, \quad \text{(S7)}$$

$$\frac{\partial B_b(\phi,t)}{\partial t} = -(\frac{\kappa}{2}+i\delta\omega_A)B_b+i\frac{D_2}{2}\frac{\partial^2 B_b}{\partial\phi^2}+\sqrt{\alpha}F_A+ig[|B_b|^2+(2-f_R)|B_p|^2]B_b+ig\tau_R D_1 B_b\frac{\partial(|B_p|^2+|B_b|^2)}{\partial\phi}+iG^*A_p. \quad \text{(S8)}$$

where, for simplicity, only a single scatterer is assumed in the cavity so that $\Gamma(\theta) = G\delta(\theta)$.

Fig. S2(b) numerically studies locking of the CP soliton repetition rates by solution of the above coupled soliton equations. By plotting the time evolution of the difference in the CP solitons' peak position ($\phi_{\mathrm{Ac}} - \phi_{\mathrm{Bc}}$) within their own moving frames, we can extract their repetition rate difference from the slope of the curves. The upper panel in fig. S2(b) shows how the solitons rate lock after a few cavity round trips. Backscatter coupling values (internal and taper) are indicated as is the pump detuning in normalized units. In the second panel, the pump detuning is increased and this leads to unlocking. However, in the third and fourth panels locking is again restored by either increasing the taper coupling or the backscatter coupling.

Finally, the measured interferogram in the rate locked condition is shown in fig. S3. The trace contains no features other than noise. Fig. 2c of the main text in which the rates are distinct and unlocked is included in fig. S3 for

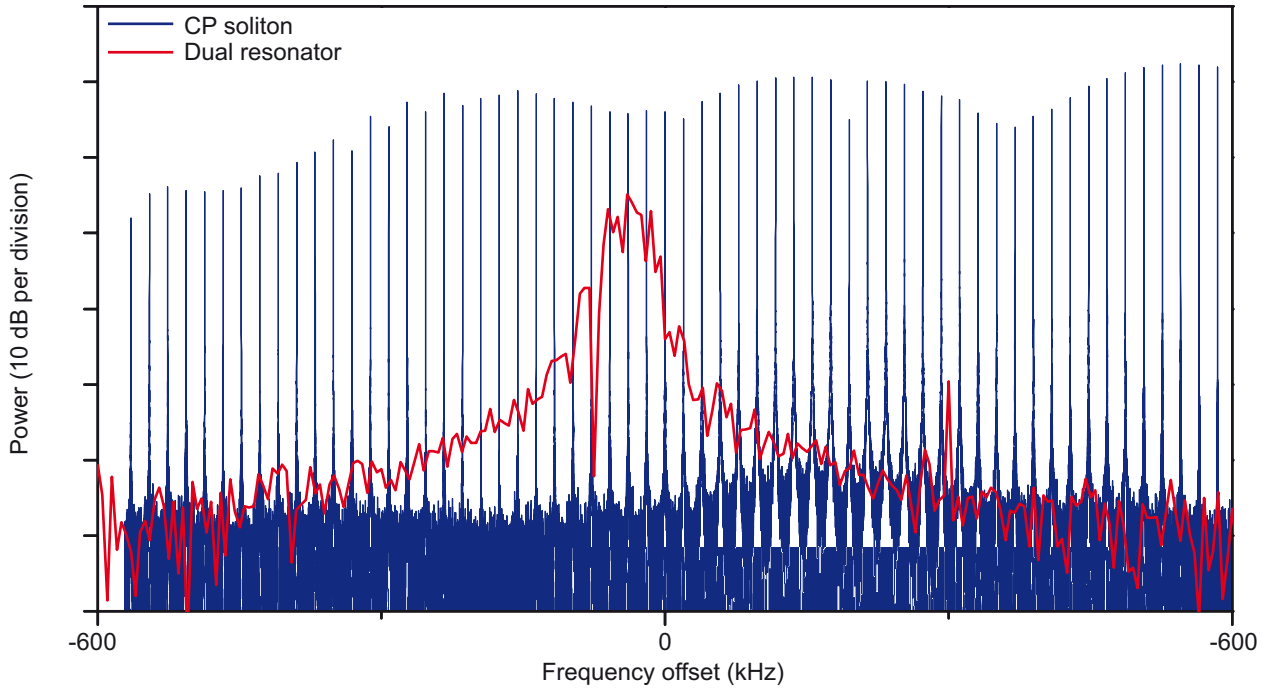

FIG. S4: Zoom-in of RF spectra showing dual soliton beatnotes. The blue trace denotes the CP solitons with integration time 50 ms. The red trace represents the results from solitons generated in two distinct microresonators with integration time 200 μs.

comparison.

III. COMPARISON BETWEEN CP SOLITON DUAL COMB AND TWO-RESONATOR DUAL COMB

Microresonator soliton dual-comb spectroscopy has recently been demonstrated using solitons generated from two distinct resonators[4]. As discussed in the main text, CP solitons eliminate the need for two resonators and also improve the stability of the interferogram spectrum through the CP soliton locking. Here we compare the dual-comb spectra from CP solitons and dual resonators. Fig. S4 overlays a zoom-in of the interferogram spectra for cases in which two, distinct resonators are used (repetition rate difference of order 1 MHz) and phase-locked CP solitons are used (repetition rate difference of order 10s of kHz). A dramatic difference in the spectral width of each individual spectral line of the CP soliton case (blue spectrum) versus the dual comb spectral line is apparent. The signal-to-noise ratio is also greatly improved for the CP soliton case. In principle, the dual comb system could be phase locked, however the locking mechanism demonstrated here is intrinsic to the physics of the counter-propagating solitons. It therefore avoids complex external locking apparatus and thereby provides a major simplification (even beyond the elimination a second frequency comb) to these systems.

[1] G. P. Agrawal, *Nonlinear fiber optics* (Academic press, 2007).
[2] Q.-F. Yang, X. Yi, K. Y. Yang, and K. Vahala, Nat. Phys. **13**, 53 (2017).
[3] X. Yi, Q.-F. Yang, K. Y. Yang, and K. Vahala, Opt. Lett. **41**, 3419 (2016).
[4] M.-G. Suh, Q.-F. Yang, K. Y. Yang, X. Yi, and K. Vahala, Science, doi: 10.1126/science.aah6516 (2016).